

Annex

The papers received after 25 January 2009.

An Investigation of Overturning Moments of Portal Frames at Elevated Temperatures	Annex 2
Rahman M., Lim J., Hamilton R., Komlekci T., Pritchard D., Xu Y., <i>United Kingdom</i>	
On the Distortional Buckling, Post-Buckling and Strength of Cold-Formed Steel Lipped Channel Columns Subjected to Elevated Temperatures	Annex 8
Landesmann A., <i>Brazil</i> , Camotim D. <i>Portugal</i> Batista E.M., <i>Brazil</i>	
PROMETHEE, the Innovative Fire Resistance Testing Centre for Structures.....	Annex 14
Robert F., Rimlinger S., Collot E., Collignon C., <i>France</i>	

AN INVESTIGATION OF OVERTURNING MOMENTS OF PORTAL FRAMES AT ELEVATED TEMPERATURES

Mahbubur Rahman^a, James Lim^a, Robert Hamilton^b, Tugrul Komlekci^b, David Pritchard^c and Yixiang Xu^a

^a Strathclyde University, Department of Civil Engineering, Glasgow, United Kingdom

^b Strathclyde University, Department of Mechanical Engineering, Glasgow, United Kingdom

^c Strathclyde University, Department of Mathematics, Glasgow, United Kingdom

1 INTRODUCTION

In the UK, single-storey steel buildings account for over half of the constructional steelwork due to its ease of fabrication and cost-efficiency. The most common of these are portal frames. One of the major disadvantages of constructional steel is its sensitivity to fire, as steel loses strength and stiffness rapidly. For this reason, fire protection is often required, which can add to the expense of structure.

In fire, the rafter often loses stability through a snap-through-buckling mechanism (see Fig. 1.). This, however, can be capable of restabilising at high deflections, when the roof has inverted. In static analysis methods, only the initial loss of stability can be determined. In fire conditions it is imperative that boundary walls stay close to vertical, so that fire is not allowed to spread to adjacent property. The current UK fire design guide (Ref.1) provided by Steel Construction Institute (SCI) provides a method for the determination of the overturning moment at the column base that must be resisted in order to prevent stability of walls. However, the method makes a number of arbitrary assumptions and does not attempt to model the true behaviour of the frame during fire, leading to very uneconomical design details. An elaborate study of the collapse mechanism using the finite element program VULCAN has been described by Song *et al* (Ref. 2, 3). Wong (Ref.4) studied the responses of industrial pitched portal frame structures in fire both experimentally and numerically. He developed a method for calculation of the critical temperature of a steel portal frame. His method is limited to determining the temperature at which the snap-through buckling of portal frame occurs, without any consideration of post-snap through behaviour. Song *et al* (Ref.2,3) continued the work of Wong and conducted a study of the behaviour of portal frames using dynamic analysis. Song investigated the failure mechanism of a single-storey haunched portal frame in fire subject to different support conditions at their column base. They pointed out that the rafter is capable of restabilising after it collapsed through snap-through-buckling mechanism. Vassart *et al* (Ref.5) presented a comparative study on a double span portal frame in fire designed by Franssen *et al* (Ref. 6). Yin *et al* (Ref.7) performed a numerical study of large deflection behaviour of restrained steel beams at elevated temperatures.

It was established that the large deflection behaviour of steel beams could significantly affect their survival temperature in fire, and they particularly emphasized the behaviour of axially restrained steel beams in catenary action. In the present paper, a non-linear elasto-plastic dynamic finite element analysis is presented that can be used to simulate the collapse of a

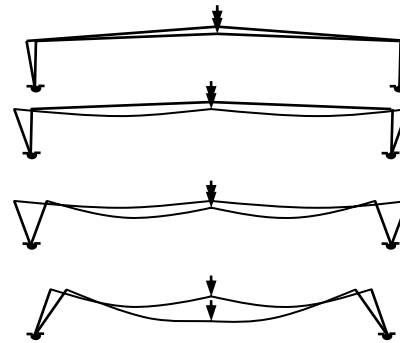


Fig. 1. Snap-through mechanism

portal frame in standard ISO834 fire (Ref. 8). The results of the dynamic model are validated through comparison against results found in the literature, and also through results obtained using the same model but solved using implicit static, implicit dynamic and explicit dynamic analyses.

It is demonstrated that an explicit dynamic analysis is a viable alternative to an implicit dynamic analysis, and has the advantage of being computationally more efficient to solve when the problem is quasi-static in nature. The implicit dynamic model is used to investigate the current UK fire design guide (Ref. 1) published by SCI.

2 MATERIAL PROPERTIES AT ELEVATED TEMPERATURE

Fig.2 shows the reduction of ultimate strength of steel at different temperatures to that at ambient temperature. As can be seen, there is no loss in ultimate strength at temperatures up to 400°C. Fig.3 shows stress-strain curves of steel at 20°C, 400°C, 600°C, 800°C and 1000°C in accordance to Eurocode 3 (Ref.8). It should be noted that there is no strain-hardening in the Eurocode curves and it is assumed in SCI method that only 6.5% of steel strength at ambient temperature is retained at while the steel is subjected to a temperature of 890°C. The coefficient of thermal expansion is assumed according to the same code. A value of 0.3 is used as Poisson's ratio for the whole analysis, and steel is considered as an isotropic material with a density of 7850.0 kg/m³.

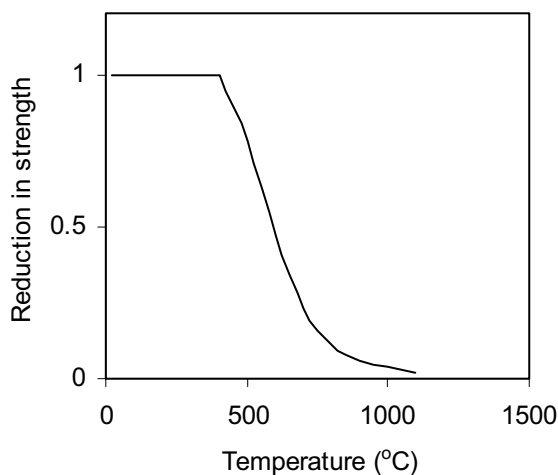


Fig.2. Variation of reduction in ultimate strength of steel against temperature

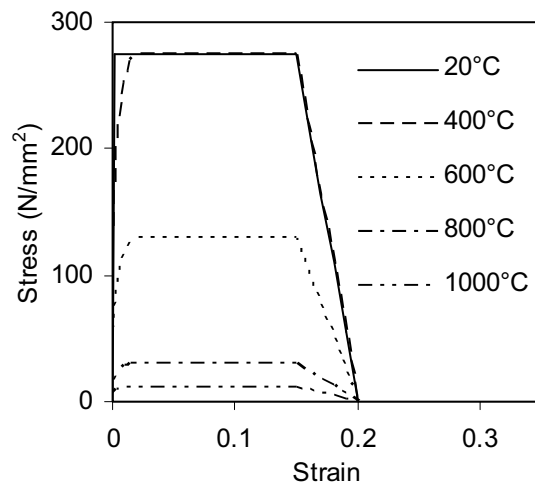


Fig. 3. Stress-strain curves for steel grade S275

3 FIRE MODEL

Fig.4 shows the standard fire rating curve (ISO834). Eurocode 3 provides a simple calculation method for calculation of section temperature while the section is unprotected or protected. The calculated temperature for an unprotected steel section IPE450 is presented in the same graph for comparison. It should be noted that ISO834 curve shows a rapid heating as compared to the section temperature based on the simple calculation method of EC3. This is because the surrounding gas temperature is assumed equal to the standard temperature while the temperature is rising inside the steel section by heat conduction and radiation.

4 BENCHMARK MODELS

The dynamic finite element model used in Section 5 of this paper needs first to be validated against the results of two benchmark models: a single span frame after Song *et al* (Ref.2) and a double span frame after Vassat *et al* (Ref.5). For both cases, non-linear elasto plastic implicit dynamic analyses were used. In the case of the analysis by Song *et al*, the finite element program VULCAN was used for the analysis. In the case of the analysis by Vassat *et al*, the general purpose finite element program ABAQUS was used.

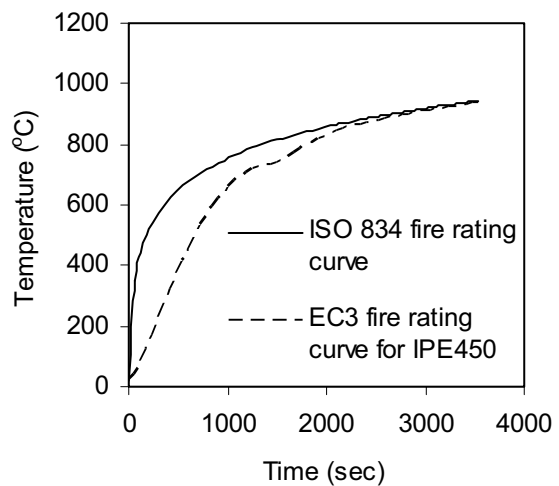


Fig. 4. Time-temperature curves

4.1 Single span portal frame

Fig.5 shows details of the single span portal frame. As can be seen, the columns of frame are pinned and the frame is loaded through a uniformly distributed load of 5.76 kN/m. The frame is modelled in ABAQUS using beam elements B21. Sixteen elements are used for each column and thirty-two elements for each side rafter.

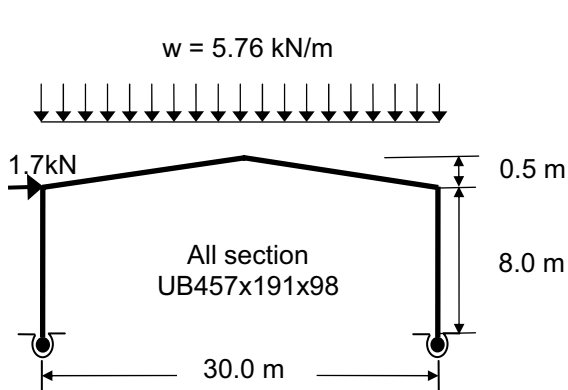


Fig. 5. Details of single span frame after Song *et al* (Ref.2)

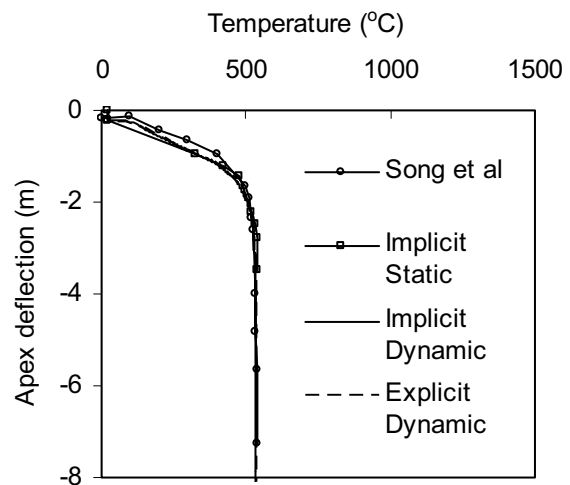


Fig. 6. Variation of apex deflection against temperature for single span frame

Fig.6 shows details of the variation of apex deflection against temperature. It can be seen that the implicit static analysis fails to converge at an apex deflection of 2.2 m when the structure starts to become geometrically unstable. The problem of geometrical instability can be overcome by using either implicit dynamic or explicit dynamic analysis. As can be seen from the same figure, the results of the implicit dynamic and explicit dynamic are similar to the results obtained by Song *et al* using VULCAN. The frame experiences snap-through-buckling at a temperature around 560°C.

4.2 Double span portal frame

Fig.7 shows details of the double span portal frame. As can be seen, temperature is increased in the left hand side rafter and column only. The right hand side column and rafter, including the middle column, are kept at ambient temperature. It can be seen from Fig.8 that only the left hand side of the portal frame will experience snap-through-buckling. Fig. 9 shows details of the variation of left hand side apex deflection against temperature. It can be seen that the implicit dynamic and explicit dynamic results are similar to results obtained by Vassart *et al.*

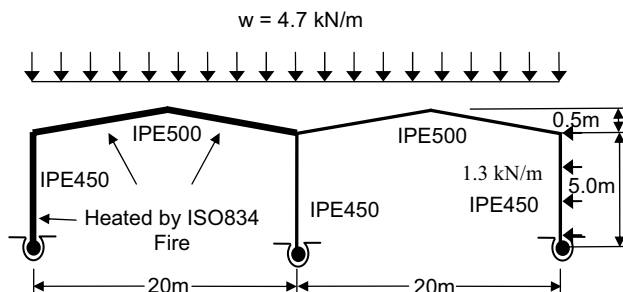


Fig.7. Details of double span frame after Vassart et al (Ref.5)

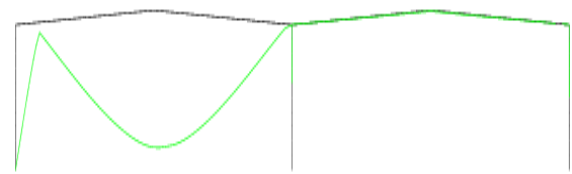


Fig. 8 Deformed shape at 1100°C (Deflections magnified by a factor of 50)

4.3 Discussion of results

For both benchmark models, it has been demonstrated that the implicit dynamic and explicit dynamic results are similar. For the purposes of the study in the following section, an implicit dynamic analysis will be adopted.

5 COMPARISON AGAINST EXISTING DESIGN RECOMMENDATIONS

The SCI have published guidelines for the design of portal frames at fire boundary conditions (Ref. 1). This method is based on calculating an overturning moment (OTM) that needs to be resisted in order to maintain

stability of the column and allow the collapse of the rafter. If this method is used, fire protection needs only be applied to the columns and the rafters can remain unprotected. Fig 10 shows the details of the portal frame analysed for comparison. Fig. 11 shows the variation of overturning moment against temperature for two frames. In the first frame, the column is unprotected, while in the second frame the column is protected. In both models the frames do not collapse at a temperature of 1100°C, with an apex deflection of less than 0.1 m. Using the SCI method, the overturning moment is calculated to be 61.3 kNm. This value of overturning moment is indicated in the same figure. As can be seen, the overturning moment obtained by the finite element model for both cases is higher than the overturning moment calculated using the SCI method. The dotted lines at 301 kN represents the plastic moment capacity of the steel section detailed in the figure.

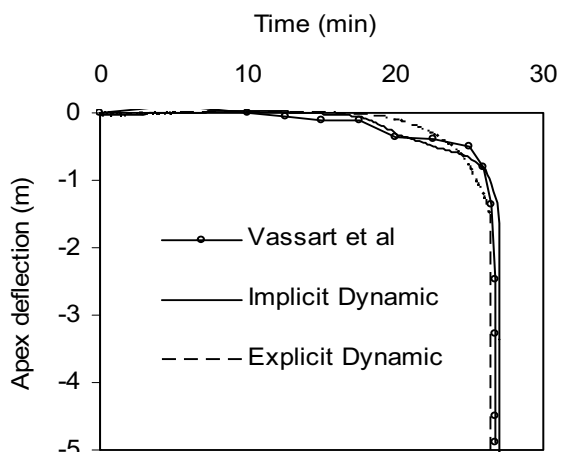


Fig. 9. Apex deflection of left rafter against time

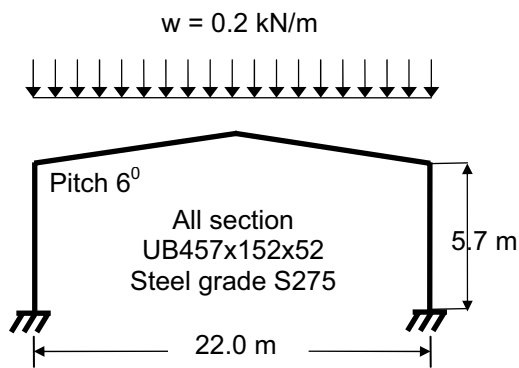


Fig.10. Details of exemplar single span portal frame after SCI (Ref. 1)

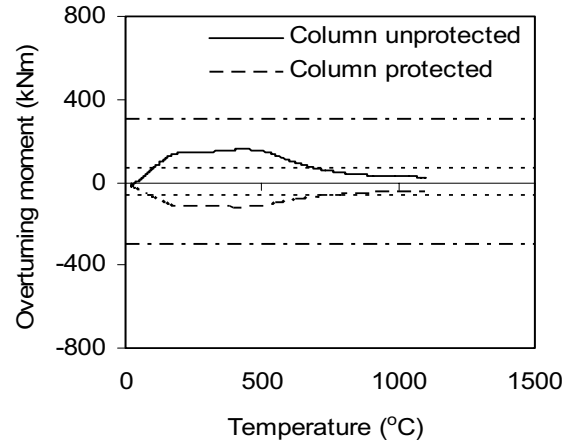


Fig. 11. Overturning moment

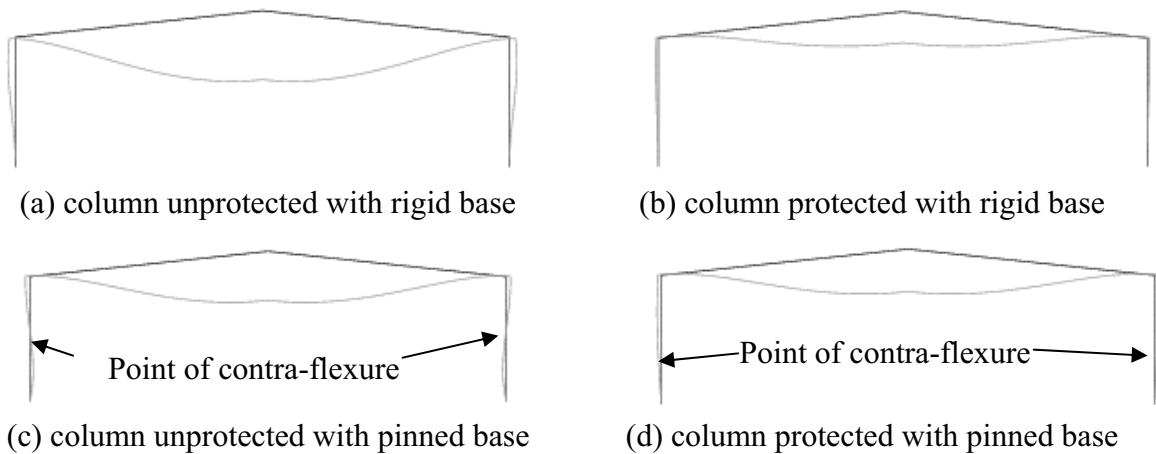


Fig. 12 Deformed shape (Deflection magnified by a factor of 25)

It is interesting to note that the reactant moment for the case of column unprotected and column protected are opposite in direction. Two further models were analysed in which the column base was pinned. The deformed shapes for all four models at 1100°C are shown in Fig.12. From deformed shape of the frames having pinned bases, it can be seen why the overturning moments act in opposite directions. One can notice the point of contraflexure in the middle of columns.

6 LOADS FOR SNAP-THROUGH BUCKLING

The frame described in the Section 5 did not undergo snap-through-buckling. In this section, the same geometry of frame has been analysed but varying the vertical uniformly distributed load from 0.5 kN/m to 5.0 kN/m. The results have been compared against the SCI model as shown in Fig 13. As can be seen, SCI method is conservative for the lower collapse load but for higher collapse load, this method overestimates the overturning moment and leads to uneconomic design of steel section. Fig 14 shows the variation of apex deflection at different temperatures with various types of loads on rafter. As can be seen from this figure, snap-through-buckling occurs for a load of around 3.5kN/m.

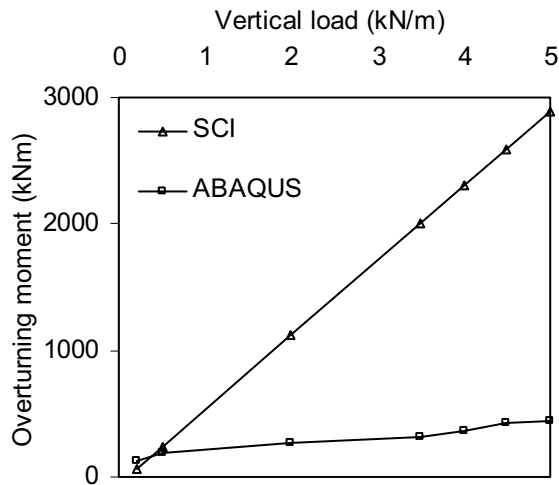


Fig. 13. Comparison of overturning moment

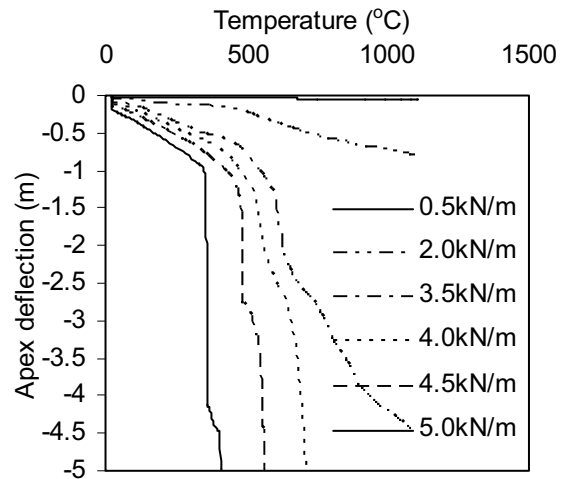


Fig. 14. Effect of different vertical loads

7 CONCLUDING REMARKS AND FURTHER WORK

Based on the present study, the following conclusion can be drawn:

- Both implicit dynamic and explicit dynamic analysis present the similar results.
- The present model is capable of predicting the post-snap-through-buckling behaviour.
- The reactant moment for the case of column unprotected and column protected are opposite in sign as point of contra-flexure is formed in the middle of column.
- The SCI OTM method can be over conservative.

In further work, the effect of axial and rotational restraints will be studied in order to determine whether they have any impact on the snap-through mechanism of the portal frame. In addition, a 3D analysis will be carried-out with a complete portal frame building.

REFERENCES

- [1] Simms W. I. and Newman G.M. (2002), "Single-storey steel framed buildings in fire boundary conditions", The Steel Construction Institute, SCI P313, Berkshire, UK.
- [2] Song Y., Huang Z., Burgess I. W. and Plank R. J. (2007) "The design of pitched-roof steel portal frames against fire", *5th Int. conf. in Steel Structures*, vol. III, pp. 728-733.
- [3] Song Y., Huang Z., Burgess I. W. and Plank R. J. (2007) "The design of pitched-roof steel portal frames against fire".
- [4] Wong Y.S. (2001), "The structural response of industrial portal frame structures in fire", PhD thesis, University of Sheffield.
- [5] Vassart O., Brasseur M., and Cajot L. G., Obiala R., Spasov Y., Friffin A., Renaud C., Zhao B., Arce C., and De la Quintana J. (2007), "Fire safety of industrial halls and low-rise buildings", Final report, Technical Steel Research, European Commission.
- [6] Franssen J.M. and Gens F. (2004), "Dynamic analysis used to cope with partial and temporary failures", Third International Workshop – Structures in Fire: paper S6-3.
- [7] Yin Y.Z and Wang Y.C. (2004), "A numerical study of large deflection behaviour of restrained steel beams at elevated temperatures", *Journal of Constructional Steel Research*, vol. 60, pp.1029-1047.
- [8] BS EN 1993-1-2:2005 Eurocode 3: Design of steel structures. Part 1-2: General rules-Structural fire design.

ON THE DISTORTIONAL BUCKLING, POST-BUCKLING AND STRENGTH of Cold-Formed Steel Lipped Channel Columns Subjected to Elevated Temperatures

Alexandre Landesmann^a, Dinar Camotim^b, Eduardo M. Batista^a

^aCivil Eng. Program, Federal University of Rio de Janeiro (COPPE/UFRJ), Brazil; E-Mail: {alandes; batista}@coc.ufrj.br

^bDepartment of Civil Eng. and Architecture, ICIST/IST, Technical University of Lisbon, Portugal; E-Mail: dcamotim@civil.ist.utl.pt

1 INTRODUCTION

Most cold-formed steel members display very slender thin-walled open cross-sections, a feature making them highly prone to instability phenomena, namely (i) local (wall transverse bending only), (ii) distortional (both wall transverse bending and cross-section distortion) or (iii) global (flexural or flexural-torsional – cross-section rigid-body motions only) buckling. In addition, members with relatively similar local-distortional-global bifurcation stresses are also liable to mode interaction phenomena. Currently, a rigorous assessment of the structural behaviour and ultimate strength of thin-walled members can only be achieved through sophisticated computer intensive shell finite element analyses. Such an assessment plays a key role in the validation and/or calibration of easy-to-use design methodologies intended for practical applications (*e.g.*, the increasingly popular *Direct Strength Method* – *e.g.*, Schafer [1]). Such methodologies can only be rational and fully efficient if based on reliable and physically sound models, stemming from an in-depth knowledge of the member structural response.

It is well-known that the use of cold-formed steel profiles in the construction of the structural framing of either industrial (predominantly) or residential buildings has been growing steadily in the last few years, mainly due to their high structural efficiency (high strength-to-weight ratio), remarkable fabrication versatility and increasingly low production and erection costs. Therefore, it is quite important to assess the structural response of such profiles when subjected to high temperatures, namely those caused by fire – this has been already extensively done for hot-rolled and welded steel members. However, the research activity devoted to cold-formed steel members under fire conditions is still rather scarce, as attested by the relatively small number of available publications – the recent works of Kaitila [2], Feng *et al.* [3,4], Lee *et al.* [5], Feng and Wang [6], Chen and Young [7-9] and, Ranawaka and Mahendran [10], deserve to be specially mentioned. Moreover, only very few of these works address members affected by distortional buckling, an instability phenomenon that often governs the behaviour and strength of lipped members.

The objective of this paper is to report the current results of an ongoing shell finite element investigation on the distortional buckling, post-buckling and ultimate strength behaviour of simply supported cold-formed steel lipped channel columns subjected to (i) concentric compression and (ii) elevated temperatures caused by fire conditions – the influence of unavoidable initial geometrical imperfections is also taken into account. The steel constitutive relation at high temperatures is taken (i) in accordance with Eurocode 3 (Part 1.2) [11] and (ii) on the basis of a cross-section temperature distribution estimated by means of a 2D non-linear heat transfer model (as a function of the elapsed fire duration). The geometrically and materially non-linear response of the cold-formed steel lipped channel columns is determined by means of shell finite element analyses performed in the commercial code ANSYS [12]. The column collapse is computed for two loading strategies, involving either (i) the application of a increasing compressive load on a column exhibiting a constant temperature distribution (*i.e.*, one obtains column *failure loads*) or (ii) the application of an initial compressive force, which remains constant, followed by a progressive temperature increase (*i.e.*, one obtains column *failure temperatures*).

2 NUMERICAL ANALYSIS

2.1 Lipped Channel Column Geometry and Buckling Behaviour

The simply supported cold-formed steel lipped channel columns analysed in this work have length $L=60\text{ cm}$ and exhibit the cross-section dimensions displayed in Fig. 1(a). This column geometry ensures the distortional nature of the column critical buckling mode – Fig. 1(b) provides an overall view of this buckling mode, which is characterised by the simultaneous presence of cross-section wall transverse bending (in-plane deformation) and rigid-body motions of the flange-lip assemblies. It is still worth

noting that the buckling analyses required to identify the above column geometry length were carried out in the freely available code *GBTUL* [13], which is based on a recently developed Generalised Beam Theory (GBT) formulation [14]. The various curves depicted in Fig. 1(c) provide the variation of the critical elastic buckling stress σ_{cr} with the column length L (in logarithmic scale) and temperature T – note that (i) T varies between $20/100^\circ\text{C}$ (“room temperature” material behaviour) and 800°C , and that (ii) σ_{cr} is normalised with respect to $\sigma_{cr,D,20}=154.9\text{ MPa}$ (minimum critical stress associated with a single half-wave distortional buckling mode at $T=20^\circ\text{C}$). One readily observes that (i) all curves may be obtained from the top one by performing a “vertical translation” with a value that depends exclusively on the Young’s modulus erosion caused by the rising temperature (Poisson’s ratio is assumed temperature-independent and equal to 0.3), and that (ii) $L=60\text{ cm}$ always corresponds to the minimum critical stress associated with a single half-wave distortional buckling mode ($\sigma_{cr,D,T}$). Moreover, note that $\sigma_{cr,D,T}$ drops by about 90% when the temperature rises from $20/100^\circ\text{C}$ to 800°C – and the steel Young’s modulus decreases from 205 GPa to 18.5 GPa .

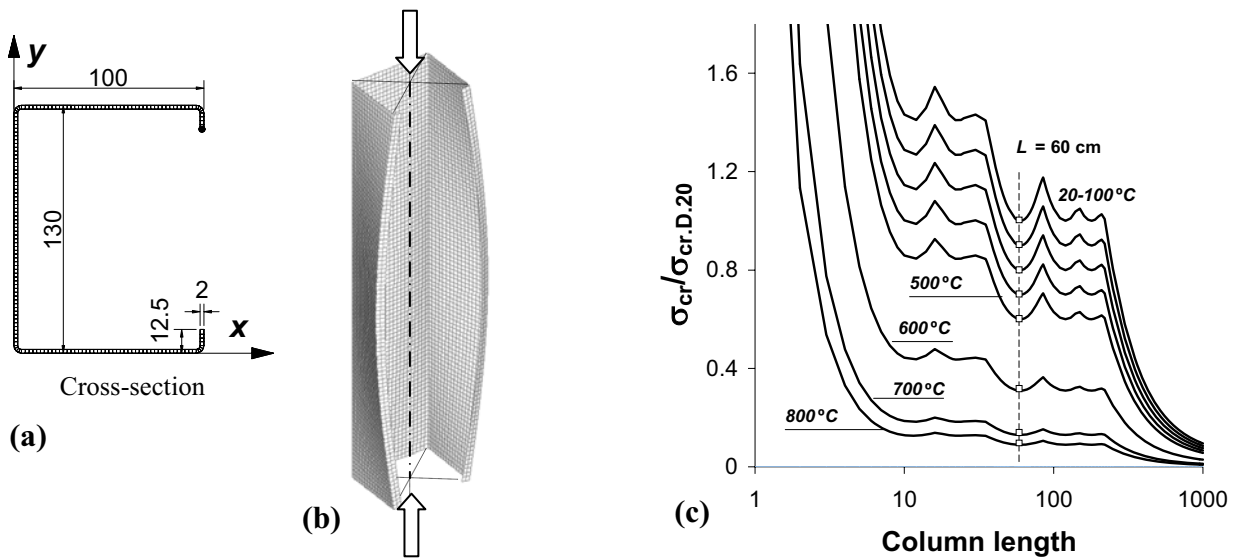


Fig. 1 – Simply supported lipped channel column (a) cross-section dimensions, (b) distortional buckling mode shape and (c) elastic buckling curves – variation of the critical buckling stress ratio $\sigma_{cr}/\sigma_{cr,D,20}$ with the column length and temperature.

2.2 Steel Material Behaviour

The columns analysed in this work are made of *S460* European standard steel ($E=205\text{ GPa}$, $f_y=460\text{ MPa}$ and $\nu=0.3$). The variation of the steel constitutive relation with the temperature is assumed to follow the model prescribed in Eurocode 3 (Part 1.2) [11]. It involves the use of three temperature-dependent reduction factors, namely k_e (Young’s modulus), k_y (yield stress) and k_p (proportional limit stress) – for temperatures above 100°C the steel stress-strain curve ceases to be bi-linear and exhibits a considerable amount of non-linear strain-hardening (thus, one must distinguish between yield and proportional limit stress).

2.3 Shell Finite Element Modelling

The distortional post-buckling and ultimate strength results reported in this work were obtained through geometrically and materially non-linear shell finite element analyses performed in the code ANSYS [12]. The columns were discretised into rather fine meshes ($6.25\text{ mm} \times 6.25\text{ mm}$ – see Fig. 1(b)) of SHELL181 elements – thin-shell four-node elements (six degrees of freedom per node) with full integration and accounting for transverse shear deformation. The column non-linear equilibrium paths presented, relating the applied stress/load to the lip vertical displacement at mid-span, were determined by means of an incremental-iterative technique employing Newton-Raphson’s method and an arc-length control strategy. All the columns analysed are simply supported (end sections locally/globally pinned that can warp freely) and the concentric compression was simulated by means of sets of equivalent nodal axial forces applied at both end sections. Moreover, all non-linear analyses incorporated column initial geometrical imperfections (i) with a critical-mode (distortional) configuration and an amplitude equal to 10% of the column wall thickness and (ii) involving outward flange-lip motions (see Fig. 1(b)).

2.4 Types of Non-Linear Analysis

Two different non-linear column analyses are performed, corresponding to different loading strategies: (i) application of a increasing compressive load on a column exhibiting a constant temperature distribution (steady case) or (ii) application of an initial compressive force, which remains constant, followed by a progressive temperature increase (transient case). In the first case, it is assumed that the initial (imperfect) column geometry already includes the thermal expansion associated with heating it to the pre-defined temperature – therefore the analyses of columns exhibiting two distinct temperatures only differ in the steel material behaviour adopted. The aim of these analyses is to determine the variation of the column *failure load* with the temperature.

In the transient case, which corresponds to a more realistic simulation of natural fire conditions, one begins by applying an axial load with a pre-defined value to an initially imperfect column at “room temperature” $T=20^{\circ}\text{C}$ (obviously, the applied load must be lower than the associated ultimate value). Then, the ensuing column deflected equilibrium state is recorded. Finally, incremental temperature increases are prescribed to the column, leading it to a neighbouring (more deflected) equilibrium state – in order to obtain the new equilibrium state, the shell finite element analysis must take into account (i) the variation of the steel stress-strain curve, (ii) the thermal strains caused by temperature rise and (iii) the continuous presence of the axial load. The aim of these analyses is to assess the variation of the column *failure temperature* with the applied load – in other words, to determine for which temperature does the applied load cease to correspond to a column equilibrium state.

2.5 Temperature Evolution

In order to obtain the evolution of the column temperature as a function of the elapsed fire duration, the 2D non-linear heat transfer finite model incorporated in the code SAFIR [15] was employed. The temperature evolution within the column cross-section (it is deemed longitudinally uniform) is calculated in accordance with the fire design curve prescribed in Eurocode 1 (Part 1.2) [16]. Since the column cross-section is deemed to be completely engulfed in flames, it is fair to assume that both the cross-section and the surrounding air share the same temperature – moreover, the above standard temperature-time curve is applicable to all the cross-section walls.

Finally, it is worth mentioning that thermal actions, including heat transfer through convection and radiation, have also been included in the analyses at constant load – since the fire duration is assumed to be small (less than 1 hour), creep effects have been neglected.

3 NUMERICAL RESULTS

3.1 Column Failure Loads at Constant Temperature

Fig. 2(a) shows the non-linear equilibrium paths of initial imperfect columns with nine uniform temperatures ranging from $20/100^{\circ}\text{C}$ (20°C is “room temperature”) to 800°C – each of them relates the applied stress σ , normalised with respect to $\sigma_{cr,D,20}=154.9\text{ MPa}$, with the (outward) vertical displacement of the mid-span lip tips. One observes that, as expected, both the column ultimate strength and ductility prior to failure decrease with T . In order to quantify the column response erosion stemming from the rising temperature, one next determines and compares the stress ratios $\sigma_{cr,D,T}/\sigma_{cr,D,20}$ (critical stress ratio), $\sigma_{u,D,T}/\sigma_{u,D,20}$ (ultimate stress ratio) and $\sigma_{u,D,T}/\sigma_{cr,D,T}$ (post-buckling strength reserve). The variation of the first two ratios with T is plotted in Fig. 2(b) – one readily concludes that the values of these two ratios practically coincide, which means that the column distortional critical and ultimate stresses are equally affected by the temperature. This fact is bound to have far-reaching design implications – recall that most design methodologies (*e.g.*, the Direct Strength Method) provide ultimate strength estimates on the basis of critical stress values. On the other hand, the values of $\sigma_{u,D,T}/\sigma_{cr,D,T}$ are all comprised between 1.04 and 1.00 , which means that, at least for this particular column geometry, the distortional post-buckling strength reserve is very small and remains virtually unaltered when the temperature increases – Ranawaka and Mahendran [10] recently reported the results of an experimental investigation that led to qualitatively similar conclusions.

Fig. 3 shows the Von Mises stress distributions occurring at the distortional collapse ($\sigma=\sigma_{u,D,T}$) of columns subjected to four different temperatures ($T=20-400-600-800^{\circ}\text{C}$) – note that the “stress scales” are different.

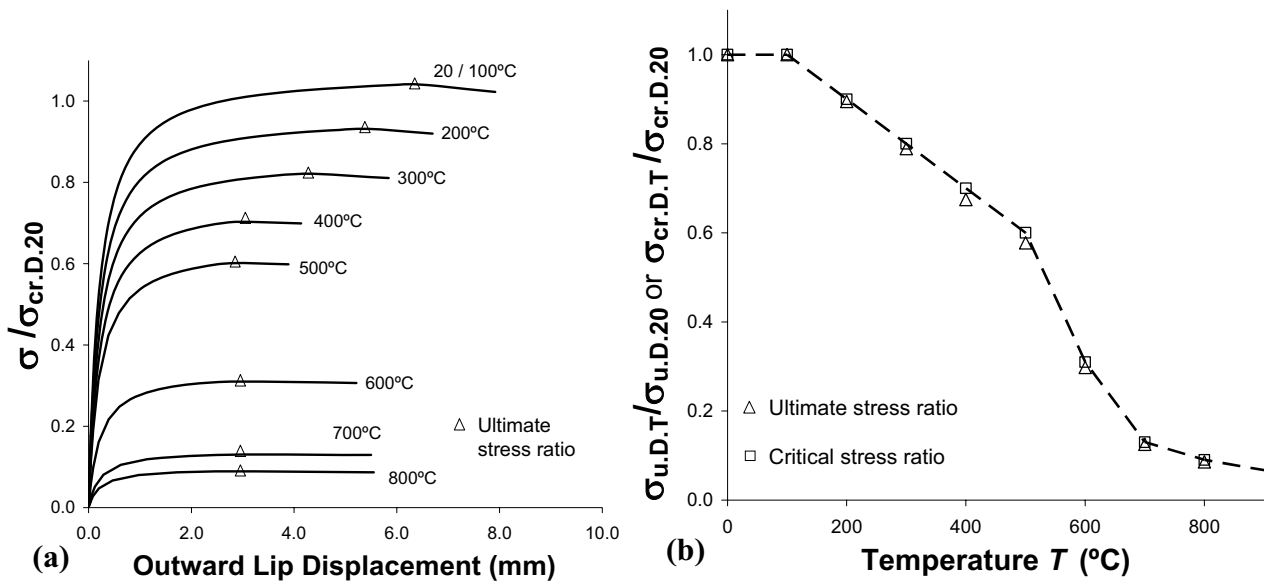


Fig. 2 – Variation with T of the column (a) post-buckling equilibrium paths and (b) critical and ultimate stress ratios.

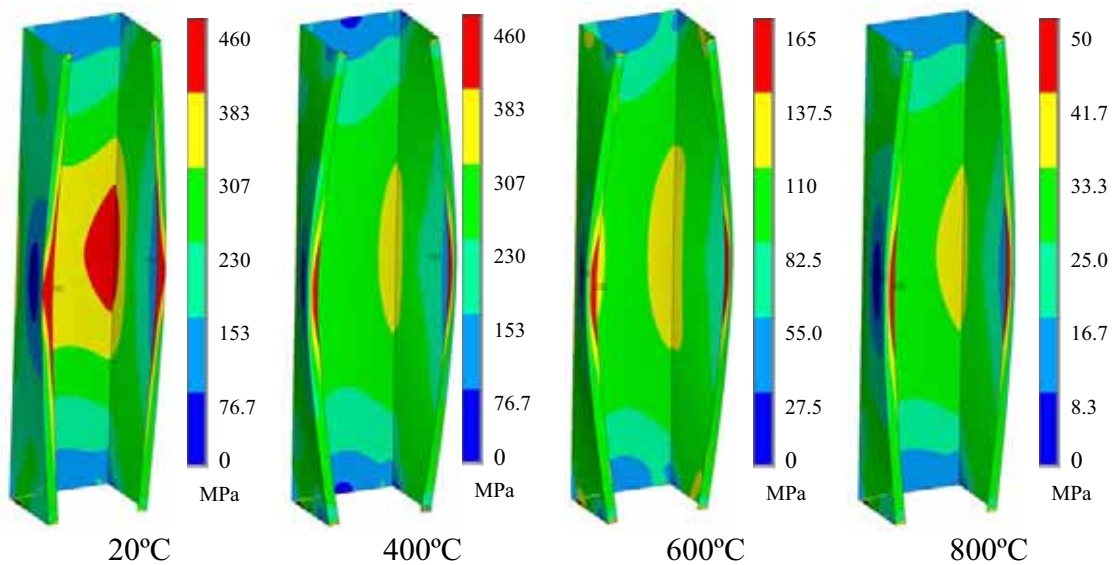


Fig. 3 – Von Mises stress distributions occurring at the distortional collapse of columns subjected to five different temperatures.

One observes that, since the thermal action effects have been neglected, the distortional failure modes are virtually identical in all the columns, *i.e.*, they do not depend on the temperature. Moreover, the Von Mises stress distributions are also qualitatively rather similar in the four columns – the higher stresses always occur in the vicinity of the lip free ends. It is worth noting that the collapse is always triggered by the yielding of the web-flange edge regions in the vicinity of the column mid-span. Quantitatively speaking, the stress values obviously decrease as the temperature rises and continuously erodes the steel material behaviour.

3.2 Column Failure Temperatures at Constant Load

The curves shown in Fig. 4(a) concern the behaviour of initially imperfect columns that (i) are first subjected to 20, 40, 60 and 80% of their distortional critical buckling load ($P_{cr,D.20}$) and (ii) subsequently acted by small uniform temperature increments (starting at $T=20^\circ\text{C}$). After each increment, one seeks a column equilibrium configuration that (i) accommodates the change in the steel constitutive (stress-strain) relationship, (ii) includes the geometry change due to the thermal strains stemming from the temperature increase and (iii) incorporates the corresponding geometrically non-linear effects associated with the (constant) applied load. The temperature is incrementally raised until no equilibrium configuration can be reached (for that applied load), which means that the column collapses for that temperature value – the *failure temperature*, which obviously drops as the load applied to the column increases. As expected, it

was observed that the column failure modes (not shown here) are virtually identical to those depicted in Fig. 3 and concerning the collapse of columns under an increasing applied load.

On the basis of the well known member temperature evolution (time-temperature relation shown in Fig. 4(b) [15]), it is possible to determine the time required for the column to fail as function of the applied load value – these “failure times” are plotted in Fig. 4(b) versus the applied load ratio $P/P_{cr.D.20}$.

An interesting question that the authors plan to address in the near future is the relation existing between the solutions of the steady state (failure loads) and transient (failure temperatures) analyses. In other words, to investigate how close is (i) the failure load at temperature T_0 ($P_{u.T_0}$) from (ii) the applied load to which corresponds a failure load also equal to T_0 . In this context, it is worth mentioning that the experimental results recently published by Ranawaka and Mahendran [10] seem to indicate that the differences between the two above load values are negligible.

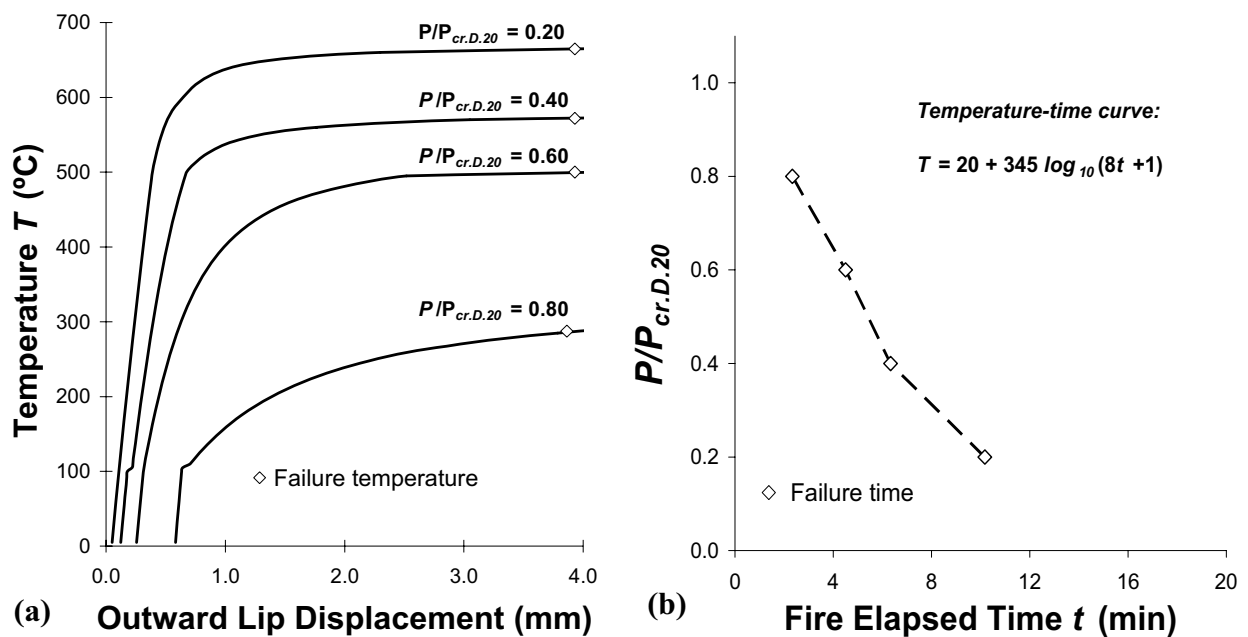


Fig. 4 –Variation with $P/P_{cr.D.20}$ of the column (a) response to a temperature increase and (b) failure time.

4 CONCLUDING REMARKS

This paper reported the available results of an ongoing shell finite element investigation on the distortional buckling, post-buckling and ultimate strength behaviour of simply supported cold-formed steel lipped channel columns subjected to (i) concentric compression and (ii) elevated temperatures caused by fire conditions. The steel constitutive relation at high temperatures was taken in accordance with Eurocode 3 and the geometrically and materially non-linear response of the cold-formed steel lipped channel columns was determined by means of shell finite element analyses performed in the code ANSYS.

The column collapse was computed for two loading strategies, involving either (i) the application of an increasing compressive load on a column exhibiting a constant temperature distribution (to obtain column *failure loads*) or (ii) the application of an initial compressive force, which remains constant, followed by a progressive temperature increase (to obtains column *failure temperatures* or, considering the member temperature evolution, column *failure times*). The column temperature evolution was obtained by means of 2D non-linear heat transfer finite element analyses carried out in the code SAFIR and adopting the fire design curve prescribed in Eurocode 1 in all the column inner and outer surfaces.

Finally, it is worth noting that a data bank of (numerically and experimentally obtained) failure loads and temperatures similar to those dealt with in this work should be very helpful in establishing guidelines for the design of cold-formed steel lipped channel columns subjected to elevated temperatures and/or fire conditions – the authors plan to pursue this avenue in the near-to-intermediate future.

REFERENCES

- [1] Schafer B., Review: the Direct Strength Method of cold-formed steel member design, *Journal of Constructional Steel Research*, **64**(7-8), 766-788, 2008.
- [2] Kaitila O., Imperfection sensitivity analysis of lipped channel columns at high temperatures, *Journal of Constructional Steel Research*, **58**(3), 333-351, 2002.
- [3] Feng M., Wang Y.C., Davies J.M., Structural behaviour of cold-formed thin-walled short steel channel columns at elevated temperatures – Part 1: experiments, *Thin-Walled Structures*, **41**(6), 543-570, 2003.
- [4] Feng M., Wang Y.C., Davies J.M., Structural behaviour of cold-formed thin-walled short steel channel columns at elevated temperatures – Part 2: Design calculations and numerical analysis, *Thin-Walled Structures*, **41**(6), 571-594, 2003.
- [5] Lee J.H., Mahendran M., Makelainen P., Prediction of mechanical properties of light gauge steels at elevated temperatures, *Journal of Constructional Steel Research*, **59**(12), 1517-1532, 2003.
- [6] Feng M., Wang Y.C., An analysis of the structural behaviour of axially loaded full-scale cold-formed thin-walled steel structural panels tested under fire conditions, *Thin-Walled Structures*, **43**(2), 291-332, 2005.
- [7] Chen J., Young B., Corner properties of cold-formed steel sections at elevated temperatures, *Thin-Walled Structures*, **44**(2), 216-223, 2006.
- [8] Chen J., Young B., Cold-formed steel lipped channel columns at elevated temperatures, *Engineering Structures*, **29**(10), 2445-2456, 2007.
- [9] Chen J., Young B., Design of high strength steel columns at elevated temperatures, *Journal of Constructional Steel Research*, **64**(6), 689-703, 2008.
- [10] Ranawaka T., Mahendran M., Distortional buckling tests of cold-formed steel compression members at elevated temperatures, *Journal of Constructional Steel Research*, **65**(2), pp.249-259, 2009.
- [11] Comité Européen de Normalisation (CEN), *Eurocode 3: Design of Steel Structures – Part 1-2: General Rules – Structural Fire Design*, Brussels, 2005.
- [12] Swanson Analysis Systems (SAS), *ANSYS Reference Manual* (vs. 8.1), 2004.
- [13] Bebiano R., Pina P., Silvestre N., Camotim D., *GBTUL 1.0 β – Buckling and Vibration Analysis of Thin-Walled Members*, DECivil/IST, Technical University of Lisbon, 2008. (<http://www.civil.ist.utl.pt/gbt>)
- [14] Bebiano R., Silvestre N., Camotim D., GBTUL – A code for the buckling analysis of cold-formed steel members, *Proceedings of 19th International Specialty Conference on Recent Research and Developments in Cold-Formed Steel Design and Construction* (St. Louis, 14-15/10) R. LaBoube, W.-W. Yu (eds.), 61-79, 2008.
- [15] Franssen J.M., Kodur V., Mason J., *User's Manual for SAFIR 2001 – Computer Program for Analysis of Structures Subjected to Fire*, 2001.
- [16] Comité Européen de Normalisation (CEN), *Eurocode 1: Actions on Structures – Part 1-2: General Actions – Actions on Structures Exposed to Fire*, Brussels, 2002.

PROMETHEE, THE INNOVATIVE FIRE RESISTANCE TESTING CENTRE FOR STRUCTURES

Fabienne Robert^a, Serge Rimlinger^a, Edmond Collot^b, Cédric Collignon^a

^a Study and Research Centre for the French Precast Concrete Industry (CERIB), Epernon, France.

^b Senior advisor

INTRODUCTION

A noticeable evolution is currently underway in the design of large structures, to enable it to be adapted to many different natural phenomena. Eco-design, risk management, developments in and multiplication of construction methods and materials, and the increasing power of digital computational resources are redefining the context of sustainable, optimized construction. Fire is still one of the most important risks for any building.

The way this is taken into account is changing noticeably, particularly through the gradual introduction of Fire Safety Engineering. Hence up till now regulations and design have been based on prescriptive considerations, mainly applied to components or unitary construction products. Fire Safety Engineering brings a new approach to designing and dimensioning structures, based on the notion of objectives. Hence it is no longer a matter of applying fixed requirements on each of the components of the structure — e.g. 1-hour fire resistance (fire stop rating) or stability, (thermal) insulation, or 1-hour smoke-tightness — but rather a question of implementing means and facilities of protection that are appropriate to pre-identified fire risks and meet defined objectives. In this design philosophy, the global behaviour of the whole structure will be taken into account, considering any kind of thermal action (fire scenario defined according to identified risks, effective fire load...).

In this context, it appears the need of a full scale facility able not only to reproduce any fire curve but also able to take into account the global behaviour of the building by the mean of reproducing interactions between the part of the structure submitted to fire and also the surrounding cold ones.

1 STANDARDS CONTEXT FOR FIRE TESTING

There is an increasing tendency for international standardization to take these new aspects into account (i.e. fire safety engineering approaches).

ISO/TR 22898:2006, “Review of outputs for fire containment tests for buildings in the context of fire safety engineering “ has been prepared in order to review whether the current ISO furnace based fire resistance testing methods remain appropriate for establishing the performance of elements of structure when exposed to fully developed fire conditions in the context of a fire safety engineered strategy for a building. It identifies whether there is a difference between the data produced and the data required. Where there is, it reviews whether the test methods can be easily adapted to improve either the relevance of the test, or the output data, to make it more suitable for use in fire engineering applications. ISO/TR 22898:2006 reviews the mechanisms and routes of fire spread and identifies the criteria used for these tests to aid simple comparison and compares them with the conditions that can lead to fire spread or a loss of tenability for people in reality.

On this basis, it makes a certain number of recommendations in terms of developments to be desired in the corresponding tests, namely:

- To be capable of controlling the forces, in particular to have control over or evaluate reacting forces on supports.

- To move towards dimensions of 6 metres in length (horizontally) and 4 metres in height.
- To reduce turbulence within furnaces.
- To monitor hot spots on the faces not exposed to the fire.
- To evaluate a structure's confinement capacity (smoke analysis and measurement of leakage rates).

These recommendations have been developed along the same lines in the TC 92/SC4/working group 12 dealing with Fire safety engineering – Performance of structures in fire ([ISO/CD 24679] under development).

With the recent advances in fire safety engineering and the opportunity for designers to take advantage of an engineering approach in evaluating the performance of structures in fire, it is becoming necessary to:

- Refine the philosophy covered by the fire safety of structures, in case of real fires, with respect to the whole structure;
- Move beyond the consideration of individual elements only and include the behaviour of the entire structural system;
- Consider realistic load conditions; and
- Include the cooling phase of the fire.

All these recommendations directed the technical choice for Promethee device.

2 OBJECTIVES AND TEST PHILISOPHY

Given the need to develop a set up able to take into account the interactions between the surrounding cold structure and the parts of the structure effectively submitted to fire, the CERIB (study and research centre for the French Precast Concrete Industry) have launched in early 2005 the project Promethee.

The two main objectives are:

- To simulate real conditions (including natural fire) in order to better assess safety levels;
- To take into account stiffness of parts of structures which are not submitted to fire (in order to have monitorable restraint levels at the edges).

How this last point has been achieved? Interactions with the surrounding cold structure are simulated by vertical jacks on corbels for bending moment at support, and by horizontal jacks. These jacks respond to the deflected shape of the structure for representative control of compressive forces, due to expansion, and of tensile forces induced by the test element's deflection.

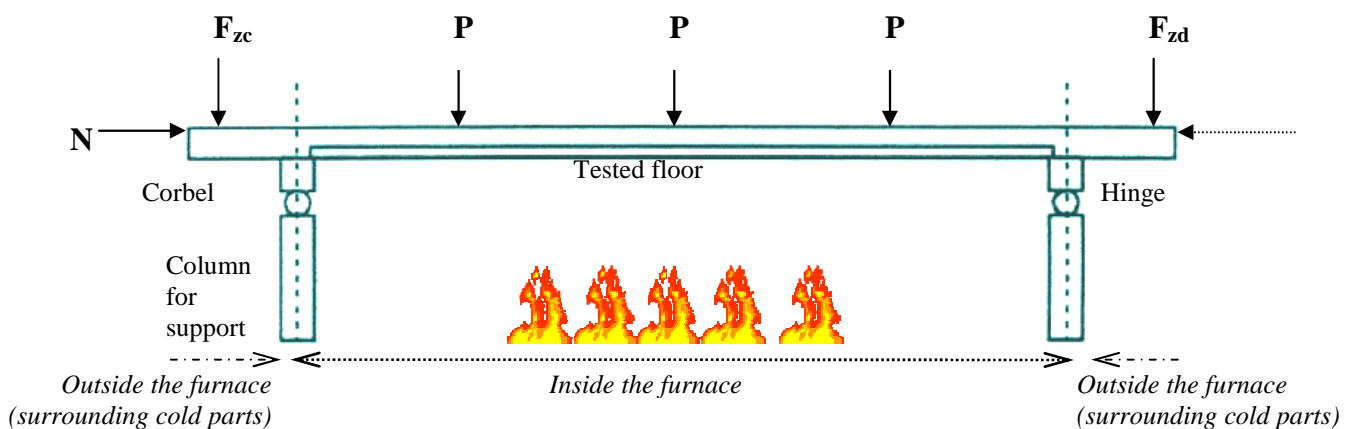


Fig. 1. Example of a floor as tested specimen

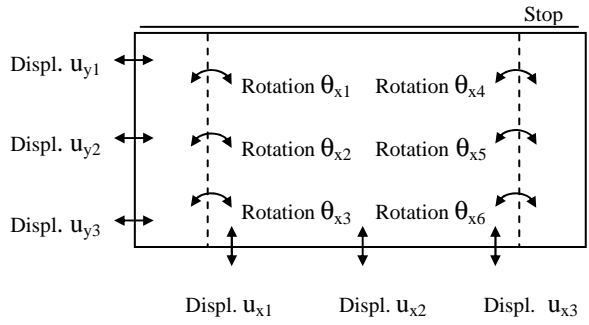


Fig. 2. Measured displacement and rotation

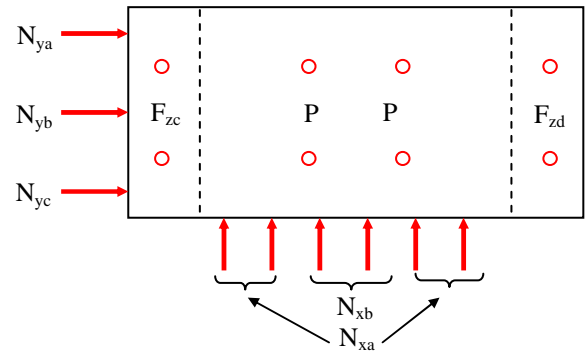


Fig. 3. Applied forces

To link the jack forces to the measured deformation that are time dependent, we use a rigidity matrix. This one is introduced before the test in the control system. It is provided by the mean of numerical simulations. These simulations, carried on software such as SAFIR or ANSYS, allow to determine bending moment/ rotation relation at support and axial forces / displacement relation at support. The stiffness coefficients are calculated through the established relations.

A simplified approach consists in considering the structural mechanics which leads to the following control matrix:

$$\begin{pmatrix} N_{xa} \\ N_{xb} \\ N_{ya} \\ N_{yb} \\ N_{yc} \\ P \\ P \\ F_{zc} \\ F_{zd} \end{pmatrix} = \begin{pmatrix} \frac{K_{xa}}{2} & 0 & \frac{K_{xa}}{2} & 0 & 0 & 0 & 0 & 0 & 0 & 0 & 0 & 0 \\ 0 & K_{xb} & 0 & 0 & 0 & 0 & 0 & 0 & 0 & 0 & 0 & 0 \\ 0 & 0 & 0 & K_{ya} & 0 & 0 & 0 & 0 & 0 & 0 & 0 & 0 \\ 0 & 0 & 0 & 0 & K_{yb} & 0 & 0 & 0 & 0 & 0 & 0 & 0 \\ 0 & 0 & 0 & 0 & 0 & K_{yc} & 0 & 0 & 0 & 0 & 0 & 0 \\ 0 & 0 & 0 & 0 & 0 & 0 & 0 & 0 & 0 & 0 & 0 & 0 \\ 0 & 0 & 0 & 0 & 0 & 0 & \frac{K_{zc}}{3} & \frac{K_{zc}}{3} & \frac{K_{zc}}{3} & 0 & 0 & 0 \\ 0 & 0 & 0 & 0 & 0 & 0 & 0 & 0 & 0 & \frac{K_{zd}}{3} & \frac{K_{zd}}{3} & \frac{K_{zd}}{3} \end{pmatrix} \begin{pmatrix} u_{x1} \\ u_{x2} \\ u_{x3} \\ u_{y1} \\ u_{y2} \\ u_{y3} \\ \theta_{x1} \\ \theta_{x2} \\ \theta_{x3} \\ \theta_{x4} \\ \theta_{x5} \\ \theta_{x6} \end{pmatrix} + \begin{pmatrix} C_{xa} \\ C_{xb} \\ C_{ya} \\ C_{yb} \\ C_{yc} \\ C_{za} \\ C_{zb} \\ C_{zc} \\ C_{zd} \end{pmatrix}$$

Fig. 4. Simplified Control matrix

Depending of the selected type of test, different kind of monitoring can be achieved. The main types of tests that can be carried out are those on connections, walls, floors, columns, beams, and tunnel lining segments.

For the connection test, there is a forced inclination of beams or purlins on each side of the connection, with a view to reproducing the actual rotation angle of the connection. In this case, the jacks for the inclination are driven in displacement. However, the jacks for shear force or compressive force on the column of the connection are driven in forces and the horizontal jacks linked to the beams or purlins on each side of the connection can be controlled either with a stiffness coefficient taking into account the axial displacement either in force obtained by numerical simulation.

3 CHARACTERISTICS OF THE SET UP

The dimensions have been established to respond to standards recommendations but also to be consistent with precast products assemblies. Thus the width of 4 m allows the assembly of three hollow cores slab element with a peripheral bond beam. The length of the furnace is 6 m, responding to the ISO/TR 22898:2006 recommendation but elements of 10 m long can be tested, partially fire exposed on 6 m, allowing to have a good representativity for deflection. A height of 4m has been chosen for walls or column.

The choice of the mechanical characteristics of the set up was made following detailed investigations into the combinations of real loads of various existing buildings, as well as from multiple digital modelling, which have made it possible to address the deformations to be expected for each unit under test envisaged. The innovative key element of the facility lies in the attention paid to taking into consideration the interactions between the cold part of the surrounding building and the hot part that is effectively subjected to the fire. This assumes that the various jacks located around unit under test are able to mechanically follow the changes in the deformation of the unit (by rotation or translation) while maintaining a level of stress.

A multidirectional loading system has been implemented through nearly 30 hydraulic jacks: 18 vertical jacks in compression (from 5 tons to 300 tons), 9 horizontal jacks (some of them are double action, from 50 to 125 tons in compression, 60 tons in tension), 2 specific vertical jacks for connection test for the inclination of beams or purlins.

The total power of the furnace is 10.8 MW, generated by 16 gas burners. A large number of fire scenarios attaining temperatures of up to 1300°C are possible, including the ISO 834 curve, the standard hydrocarbon curve, and the modified hydrocarbon curve.

Consideration has been paid to the observation of the specimen during the test. This has been achieved by endoscopic viewing of the test element during the test.

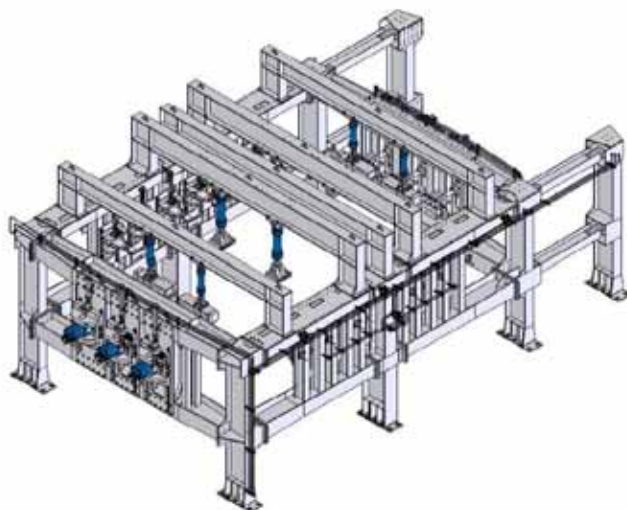


Fig. 5. Promethee diagram



Fig. 6. Photography of Promethee set up

Promethee also has a conditioned chamber, 160m², for storing test elements under conditions of 23°C and 50% relative humidity in order to attain the correct water balance.

At last, Promethee is equipped with a travelling crane of 25 tons capacity.

4 EXAMPLES OF TESTS

For the time being a series of acceptance tests has been performed to evaluate the capabilities of the set up. Walls, floors, connections, columns have been tested under different fire scenarios.

To illustrate this step, the results of a floor test are indicated below. Prestressed concrete floor 5cm high have been used with a compression slab, the total depth of the floor was 16 cm. The control matrix has been determined considering a building of 5 identical spans (5.6 m long), whose central cell is exposed to a ISO fire.

During the test, a first phase corresponds to the thermal dilatation of the floor which induces the rising of the horizontal axial forces. Due to the deflection at around 90 minutes (see on figure 8, the deflection at the mid of the span Z8 will reach 9 cm), the axial force will gradually decrease. The test has been stop after three hours of testing without having attained the critical parameters for failure.

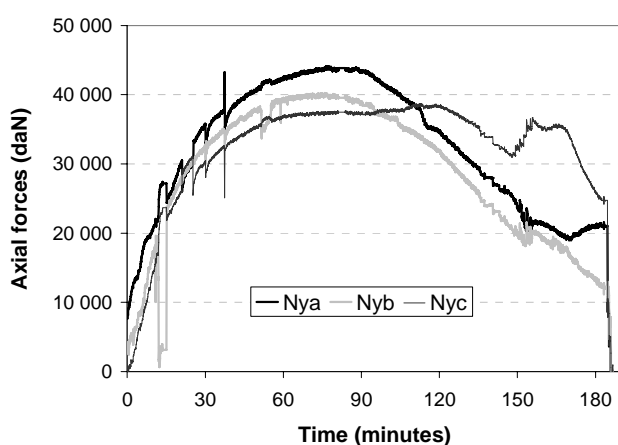


Fig. 7. Horizontal Axial forces

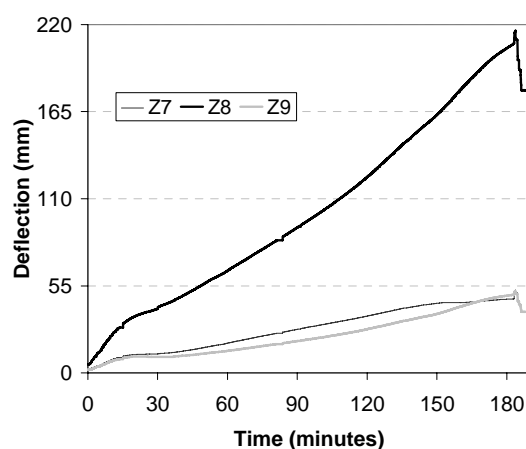


Fig. 8. Deflection



Fig. 9. Setting of the specimen



Fig. 10. View of the test

5 CONCLUSION

Promethee, a testing centre for research and development, helps give a better overall view of the level of structural safety under fire conditions. It complements the multi-scale approach CERIB has developed at its Fire Centre, via a range of tests and numerical modelling tools.

The furnace, equipped to generate a multitude of fire scenarios, is fitted with a mechanical-loading frame that reproduces interactions between the parts of a structure under testing and others unexposed to fire. These interactions are simulated by controlled, quantifiable multidirectional loading in the test element.

Promethee represents an essential factor in the understanding of how structures react in a fire. This is fundamental for ensuring life safety during evacuation or intervention by emergency services, and also for safeguarding property. Promethee is perfectly consistent with fire-safety engineering studies carried out in France, Europe, and throughout the world, and can help towards their future development.

6 REFERENCES

[ISO/TR 22898:2006] “Review of outputs for fire containment tests for buildings in the context of fire safety engineering”, technical recommendations established by ISO/TC92/SC2/WG7

[ISO/CD 24679] “Fire safety engineering - Performance of structure in fire”, under development inside ISO/TC92/SC4/WG12

